## A-1.5.1 Heterogeneous chemistry of chlorine contained molecules and radicals

**Contact person** Takashi Imamura
Team Leader
Ozone Layer Research Team
Global Environment Research Group
National Institute for Environmental Studies
Environment Agency
16-2 Onogawa, Tsukuba, Ibaraki, 305-0053, Japan
Phone +81-298-50-2406, Fax +81-298-50-2579

**Total Budget for FY1996 - FY1998** 39,171,000 Yen (FY1998 ; 13,003,000 Yen)

**Abstract:** (1) A new detector of chlorine molecule using a spectroscopic method was developed. The characteristics of the detector are the following: (i) $Cl_2$ molecule can be detected by monitoring the UV emission at 257 nm following the excitation by the Kr resonance line (123.6 nm). (ii) $Cl_2$ can be detected in air. (iii) The most effective condition for the total pressure of air is 150 Torr. (iv) The linearity of the signal is guaranteed up to 100 ppmv of $Cl_2$ in air. (v) The detection limit is about 10 ppbv for 60 s accumulation. (vi) The interference from other atmospheric trace gases seems to be negligible. (2) The uptake coefficients of $I_2$ and NO onto aqueous solution were measured by using an impinging flow reactor and determined to be $2 \times 10^{-4}$ and $< 2 \times 10^{-4}$, respectively. The uptake of acetone onto sulfuric acid was investigated using a wetted-wall flow reactor and was found to be limited by solubility. (3) Photodissociation of methyl iodide in the atmospheric window region, 190-210 nm, was investigated by using a time-resolved photoionization mass spectrometer. It was found that HI molecule as well as $CH_3$ and I was produced in the laser photolysis at 193 nm. The formation yield of HI was determined to be $0.4 \pm 0.1$.

**Key Words** heterogeneous reactions, chlorine molecule, uptake coefficient, solubility, methyl iodide

### 1. Introduction

Ozone destruction in the stratosphere is caused by catalytic cycles in the gas phase involving HOx, NOx, ClOx, and BrOx radical groups. It has been recognized that the ozone destruction efficiency is influenced not only by gas phase reactions but also by heterogeneous reactions. For example, heterogeneous reactions occurring on polar stratospheric clouds (PSCs) play an important role in polar ozone destruction. The enhancement of ozone depletion observed after the eruption of Mt. Pinatubo is thought to be a different instance to demonstrate the impact of heterogeneous processes on stratospheric ozone. However, the role of heterogeneous reactions in the stratospheric ozone destruction have not yet been well-understood. To assess the contribution of heterogeneous processes to the stratospheric ozone depletion, the following investigations are required: (1) the development of a new sensitive detector of a key species, such as $Cl_2$, (2) the measurements of uptake coefficients and the clarification of mechanisms of heterogeneous reactions, and (3) the rates and mechanisms of reactions related to aerosol formation in the stratosphere.

In the present work, the development of a $Cl_2$ detector, measurements of uptake coefficients of $I_2$, NO, and acetone onto aqueous and sulfuric acid solution, and the determination of the photodissociation yield of $CH_3I$ were carried out.

## 2. Development of $Cl_2$ detector

### 2.1. Introduction

Chlorine molecule ($Cl_2$) plays an important role in ozone chemistry, particularly in the formation mechanism of ozone hole in the Antarctic. $Cl_2$ is thought to be produced by heterogeneous reactions on PSCs, such as :

$$ClONO_2 + HCl \rightarrow Cl_2 + HNO_3$$

$$HOCl + HCl \rightarrow Cl_2 + H_2O$$

and released into the gas phase.[1] $Cl_2$ is easily photolyzed by ultra-violet (UV) radiation (300-400 nm) emitting Cl atoms into the atmosphere, However, due to the lack of a direct detection method of $Cl_2$ with a high sensitivity, our understanding on their heterogeneous reactions is limited; for example, no direct evidence on the production of $Cl_2$ in the stratosphere has not yet been provided. In this study, a new $Cl_2$ detector using a fluorescence method has been developed. This detector is expected to be used in the laboratory experiments and the field observations after some improvements.

### 2.2. Detection method

$Cl_2$ absorbed the Kr resonance line at 123.6 nm, which was assigned to the transition $2^1\Sigma_u^+(v'=3) \leftarrow X^1\Sigma_g^+$. Fig.1(a) shows the fluorescence of $Cl_2$ in the vacuum-ultra-violet(VUV) region when the light of the Kr resonance lamp irradiated the pure $Cl_2$ gas. This spectrum is assigned to two emitting transitions: $2^1\Sigma_u^+(v'=3) \rightarrow X^1\Sigma_g^+$ in 123.6-132 nm and $1^1\Sigma_u^+ \rightarrow X^1\Sigma_g^+$ in 132-210 nm. The $1^1\Sigma_u^+$ state is probably produced by an internal conversion. Moreover, when $N_2$ was added into the $Cl_2$ gas, such fluorescence was shifted from the VUV region and concentrated on the UV region around 250 nm (the transition $^3\Pi_g \rightarrow {}^3\Pi_u$) shown in Fig.1(b) due to the intersystem crossing. When $O_2$ was added in place of $N_2$, such change in emission could not be observed but the marked reduction of emission intensity was observed in the wavelength region of 137-175 nm(Fig.1(c)). The loss of the emission intensity in VUV region is due to the strong absorption by $O_2$ (Schumen-Runge band). NO efficient fluorescence quenching by $O_2$ was observed. In air, it is expected that the emission of $Cl_2$ can be observed at 257 nm where the absorption by $O_2$ is negligible. This indicates that $Cl_2$ can be detected in air by monitoring the 257 nm emission following the 123.6 nm excitation.

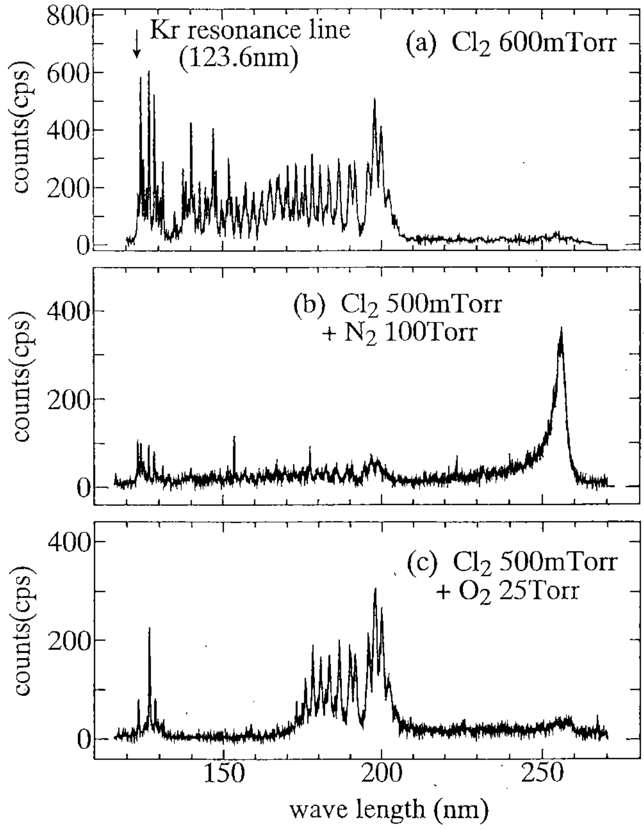


Fig.1 : Emission spectra of $Cl_2$ when Kr resonance line (123.6nm) irradiates. (a) $[Cl_2]$= 600 mTorr, (b) $[Cl_2]$=500 mTorr, $[N_2]$=100 Torr, (c)$[Cl_2]$=500 mTorr, $[O_2]$ =25Torr.

### 2.3. $Cl_2$ Detector

The $Cl_2$ detector consists of a Pyrex cell with a quartz window, a Kr resonance lamp with a $MgF_2$ window, and a solar blind photomultiplier combined with a narrow bandpass filter for the

Hg line at 253.7 nm.

**2.4. Characteristics of the detector**

(1) When $N_2$ is used as a buffer gas, the signal intensity is proportional to the total pressure. However, in air, it decreases over a given range of the total pressure, due to the absorption of the Kr resonance line (123.6 nm) by $O_2$ ($\sigma$=3.8×$10^{-19}cm^2$). The total pressure of air to detect $Cl_2$ most effectively was determined to be 150 Torr.

(2) The plot of the count rate of the signal as a function of the concentration of $Cl_2$ is shown in Fig.2. The measurement was carried out under a total pressure of air of 150 Torr. A linear relationship between the count rate and the concentration was observed. It was found that the linearity of the signal intensity was guaranteed up to 100ppmv of $Cl_2$ in air.

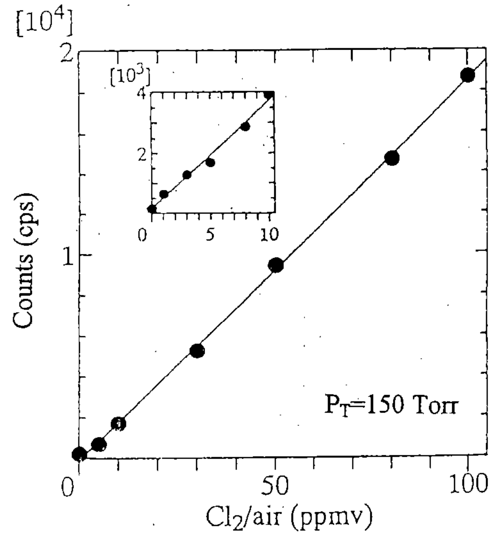


Fig.2 : Correlation of the signal with the $Cl_2$ concentration.

(3) In order to check the detection limit, we used the following reactions :

$Cl_2 + h\nu \rightarrow 2\,Cl$

$CH_4 + Cl \rightarrow CH_3 + HCl$

$CH_3 + O_2 + M \rightarrow CH_3O_2 + M$

A 6-$m^3$ photochemical chamber with a solar simulator was used to determine the detection limit of $Cl_2$. To produce low concentration of $Cl_2$, the following reactions were used:

$Cl_2 + h\nu \rightarrow 2\,Cl$

$CH_4 + Cl \rightarrow CH_3 + HCl$

$CH_3 + O_2 + M \rightarrow CH_3O_2 + M$

The pressure of air in the chamber was 150 Torr. $Cl_2$(1ppmv) as well as $CH_4$(25ppmv) were introduced into the chamber. Figure 3 shows the time profile of emission intensity. The emission intensity was slowly decayed even under the dark condition, probably due to a wall loss of $Cl_2$. A faster decay was observed when the gas mixture was photo-irradiated. After 90 minutes of irradiation, the concentration of $Cl_2$ was reduced down to 50ppbv. From the fluctuation of the signal, the detection limit was estimated to be about 10ppbv (about $10^{11}cm^{-3}$) for 60s accumulation. The sensitivity of the detector is now limited by the large background signals which probably originate the scattered light and the fluorescence from the Pyrex cell. Hence, if the detection limit will improve 1 or 2 orders, these unfavorable signals can be reduced sufficiently.

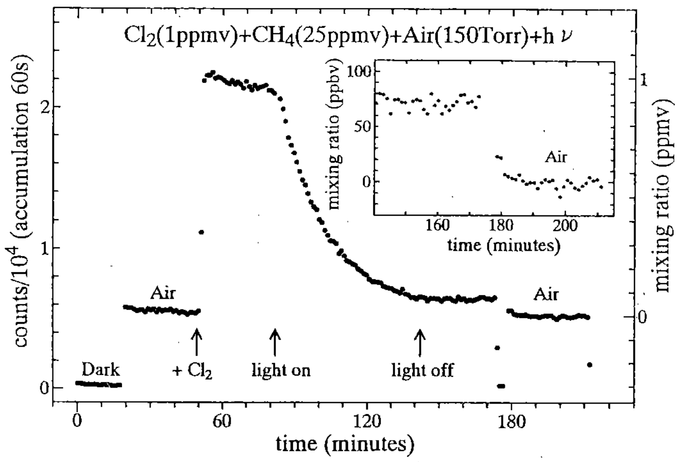


Fig.3 : Time profile of $Cl_2$ concentration for $Cl_2$ + $CH_4$ + Air(150Torr) + hν system.

(4) To check the selectivity of the $Cl_2$ detector, the fluorescence intensity near 250 nm was monitored by introducing other atmospheric trace gases into the detector and irradiating the Kr resonance line to the gas. It appears that $H_2O$, $CO_2$, $CH_4$, CO, NO, $SO_2$, and $O_3$ and their photo-fragments have no fluorescence near 250 nm. The fluorescence from the γ and β bands of NO was detected when $N_2O$ and $NO_2$ were investigated, however such fluorescence from NO fragment was completely quenched under 150 Torr of air. The fluorescence of CS and

$CF_3$ produced respectively by the photolysis of $CS_2$ and $CF_3Cl/CF_3Br$ was not completely quenched under this pressure. However, the interference by these compounds is expected to be quite small because of their low concentration (≦ 5pptv) in the atmosphere. These experimental results indicate that the developed detector can detect $Cl_2$ selectively.

### 2.5. Summary

A new and high-sensitive detector of the chlorine molecule using the fluorescence method has been developed. The characteristics of this detector are the following : (1) The most effective condition for the total pressure is 150 Torr. (2) The linearity of the signal is guaranteed up to 100ppmv of $Cl_2$ in air. (3) The detection limit is about 10ppbv for 60s accumulation. (4) The interference from other trace constituents in the atmosphere seems to be negligible.

## 3. Uptake process of acetone on sulfuric acid

### 3.1. Introduction

Acetone is now recognized as one of HOx source in the lower stratosphere and upper troposphere (LS/UT). Recently, a new heterogeneous reaction, the sulfate-mediated conversion of acetone to 4-methyl-3-penten-2-one (MPO) and trimethylbenzene (TMB), was reported.[2] The authors pointed out that the sulfate particles should be a potential reactive sink of acetone in LS/UT if reactive uptake occurs. Since the rate of proposed reaction is thought to be proportional to the square or cubic of the acetone concentration in the solution, the solubility of acetone in sulfuric acid is important. In this work, the uptake of acetone on sulfuric acid solution was observed to determine the solubility and to clarify whether the uptake is reactive or not.

### 3.2. Experimental

Most of the experiments were carried out using a rotating wetted wall flow reactor. A cylindrical reactor containing small amount of sulfuric acid (about 1cm$^3$) was rotated inside of a jacketed cylinder to coat the reactor wall with liquid. Water vapor was added to the carrier gas (He) to match the partial pressure of water over the solution. This made it possible to keep the concentration of acid be constant during an experiment. The gaseous species, such as acetone, MPO, and TMB, were monitored by a photoionization or a chemical ionization mass spectrometer.

### 3.3. Results and discussion

Fig.4 shows the variation of gaseous acetone as a function of time during absorption into and evaporation from 60 wt% $H_2SO_4$ at 250K. The dotted line in the figure shows a small decrease with time due to variation of acetone from the source. The integral of the signal over time below or above the base signal (dotted line) corresponds to the amount of acetone absorbed into or evaporated from the solution , respectively. As can be seen in the figure, the decreased signal in the absorption cycle recovers slowly with time as the liquid filled to the saturation level and the signal increased in the evaporation cycle decays to the base level as the dissolved gas was fully evaporated from the liquid. Furthermore, the amount of acetone absorbed is equal to that

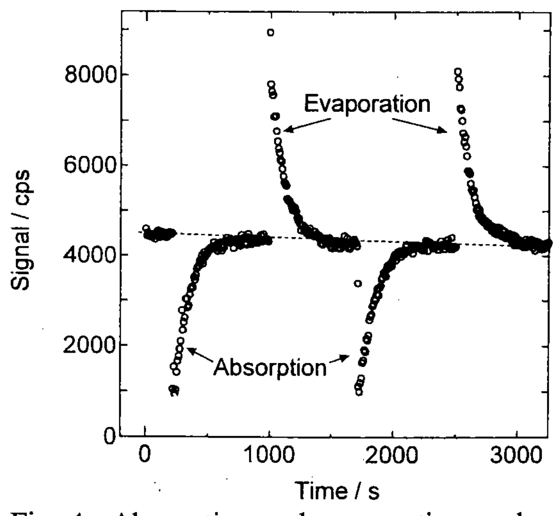


Fig. 4 : Absorption and evaporation cycles of acetone on 60 wt% of sulfuric acid at 250 K.

evaporated within the experimental error (<10%). These indicate that the uptake of acetone into 60 wt% $H_2SO_4$ at 250K is reversible and reactive loss is negligible. The Henry's law solubility of acetone in 60 wt% $H_2SO_4$ at 250 K was determined to be $5.6 \times 10^3$ M $atm^{-1}$.

Similar reversible absorption-evaporation cycle was observed in 50-80 wt% $H_2SO_4$ at 230-270K. The possible products of the proposed reaction of acetone in sulfuric acid, MPO, and TMB were not detected. These findings suggest that the reactive uptake would not be important under our experimental condition. Since the reaction rate constant in the solution should have a positive temperature dependence and the temperature in LS/UT region is lower than that in our experimental conditions, sulfuric acid aerosols in LS/UT region could not mediate the conversion of acetone to MPO and TMB efficiently.

Since the uptake of acetone on sulfuric acid solution is reversible and its solubility is low, the heterogeneous loss of acetone would not be significant in LS/UT.

## 4. Photodissociation of $CH_3I$ in the atmospheric widow region

### 4.1. Introduction

Methyl iodide ($CH_3I$) is the most dominant iodine compound in the atmosphere and is mainly released from the ocean. Its tropospheric lifetime is short, about 4 days, due to photolysis forming $CH_3$ and I. In spite of its short lifetime, a part of methyl iodide is transported into the upper tropospheric and lower stratospheric region. [3] Methyl iodide has two absorption bands; one is in the UV region and is broad feature and the other is in the wavelength region shorter than 200 nm and is banded structure.[4] In the lower stratosphere, the intensity of the solar light in the vacuum UV atmospheric window region, 190 - 210 nm, becomes strong. The character of the absorption band in the atmospheric window region is 6s $\leftarrow$ n Rydberg transition and is different that in the UV region, the $\sigma^* \leftarrow$ n valence transition. Hence, the photodissociation processes in the atmospheric window region would be different from that in the UV region. In this work, photodissociation processes were investigated by a photoionization mass spectrometer.

### 4.2. Experimental

A photoionization mass spectrometer was used to detect the photodissociation products. A Kr resonance lines (10.03 and 10.64 eV) were used as a source of photoionization. Photolysis was carried out by use of a 193 nm ArF excimer laser.

### 4.3. Results and discussion

As the photodissociation products at 248 nm, $CH_3$ and I fragments were detected. On the other hand, the products spectrum in photolysing methyl iodide at 193 nm gave a different feature as shown in Fig. 5. The spectrum was obtained by subtracting the signal observed for 2 ms before the photolysis from that observed after the irradiation. As can be seen in Fig. 5, a new ion peak appeared at m/e = 128, which should be assigned to $HI^+$. To make it clear whether HI is produced directly by photolysis or indirectly by secondary reactions, the time profiles of $HI^+$ signal as well as $CH3^+$ and $I^+$ were measured. $HI^+$ signal raise rapidly after the photolysis as $CH_3^+$ and $I^+$ signals did. The raise time of HI+ signal was much shorter than that expected if HI is formed by the

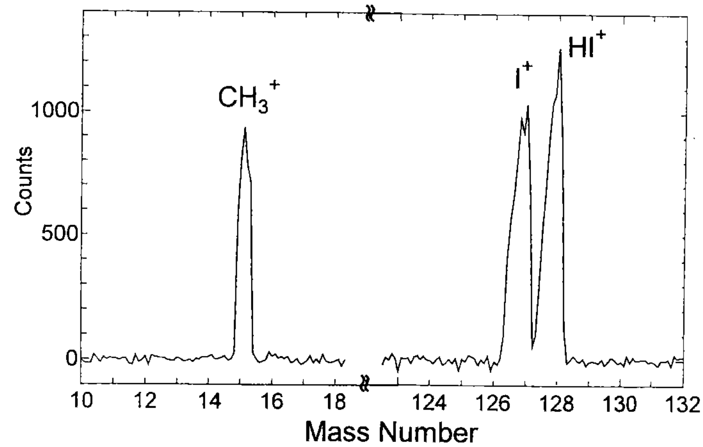

Fig. 5: Mass spectra of photodissociation products of $CH_3I$ at 193 nm.

secondary reactions, such as H + $CH_3I$. Hence, it could be concluded that HI was formed directly by 193 nm photolysis. The HI formation yield in the 193 nm photolysis was determined to be 0.4 ± 0.1 by using the detection sensitivity of HI, laser fluence, and absorption cross section of $CH_3I$ at 193 nm. This indicates that HI formation channel can compete to the process forming $CH_3$ + I. HI formed by the photolysis in the atmospheric window region would be photolysed, reacts with OH and Cl, or plays a role as a condensation nuclear in the stratosphere.

Other iodine compounds, such as $C_2H_5I$, $CH_2I_2$, and $CH_2ICl$ have a Rydberg absorption band in the atmospheric window region. The experimental results in this work suggest that the photolysis of these other iodine compounds in the window region would be different from that in the UV region and is expected to produce HI, $I_2$, and ClI.

**References**


1 S. Solomon, *Rev. Geophys.*, **26**, 131 (1988).

2 J. L. Duncan, L. R. Schindler, and J. T. Roberts, *Geophys. Res. Lett.*, **25**, 631 (1998).

3 D. Davis, J. Crawford, S. Liu, S. McKeen, A. Bandy, D. Thornton, F. Rowland, and D. Blake, *J. Geophys. Res.*, **101**, 2135 (1996).

4 A. Fahr, A. K. Nayak, and M. J. Kurylo, *Chem. Phys.*, **197**, 195 (1995).